Applied Physics Letters

Multi-line lasing in the broadly tunable ammonia quantum cascade laser pumped molecular laser

Cite as: Appl. Phys. Lett. **120**, 081108 (2022); https://doi.org/10.1063/5.0079219
Submitted: 18 November 2021 • Accepted: 09 February 2022 • Published Online: 24 February 2022

Paul Chevalier, Arman Amirzhan, Jeremy Rowlette, et al.

Applied Physics Letters ARTICLE scitation.org/journal/apl

Multi-line lasing in the broadly tunable ammonia quantum cascade laser pumped molecular laser

Cite as: Appl. Phys. Lett. **120**, 081108 (2022); doi: 10.1063/5.0079219
Submitted: 18 November 2021 · Accepted: 9 February 2022 ·
Published Online: 24 February 2022

Paul Chevalier,[1] Arman Amirzhan,[1] Jeremy Rowlette,[2] H. Ted Stinson,[2] Michael Pushkarsky,[2] Timothy Day,[2] Federico Capasso,[1,a)] and Henry O. Everitt[3,4,a)]

AFFILIATIONS

[1]Harvard John A. Paulson School of Engineering and Applied Sciences, Harvard University, Cambridge, Massachusetts 02138, USA
[2]DRS Daylight Solutions, San Diego, California 92128, USA
[3]DEVCOM Army Research Laboratory-South, Houston, Texas 77005, USA
[4]Department of Physics, Duke University, Durham, North Carolina 27708, USA

[a)]**Authors to whom correspondence should be addressed:** capasso@seas.harvard.edu and everitt@phy.duke.edu

ABSTRACT

Gaseous ammonia has previously been demonstrated as a compelling gain medium for a quantum cascade laser pumped molecular laser (QPML) exhibiting good power efficiency. Here, we explore the potential of the ammonia QPML to produce powerful, broadly tunable terahertz frequency lasing on rotational and pure inversion transitions. After theoretically predicting possible laser frequencies, pump thresholds, and efficiencies, we experimentally demonstrate unprecedented tunability—from 0.763 to 4.459 THz—by pumping Q- and R-branch infrared transitions with widely tunable quantum cascade lasers. We additionally demonstrate two types of multi-line lasing: simultaneous pure inversion and rotation–inversion transitions from the same pumped rotational state and cascaded lasing involving transitions below the pumped rotational state. We report single frequency power levels as great as 0.45 mW from a low volume laser cavity.

The quest for powerful, tunable, and continuous wave sources of terahertz radiation for use in spectroscopy, communications, imaging, and radar has recently been accelerated by the development of a new type of source: a quantum cascade laser-pumped molecular laser (QPML).[1–3] A molecular gas in a compact laser cavity can be made to lase on any rotational transition of virtually any molecule that has a permanent electric dipole moment, vapor pressure, and an infrared (IR) rotational–vibrational absorption band that may be spanned by a tunable quantum cascade laser (QCL).[1] By tuning the QCL frequency to coincide with any such rovibrational transition $J_L \rightarrow J_U$, it has been previously shown that two rotational population inversions may be created: the direct transition between $J_U \rightarrow J_U - 1$ of the excited vibrational level and the refilling transition between $J_L + 1 \rightarrow J_L$ of the ground vibrational level.[1,4] The length of the cavity containing the gas may then be adjusted so one of its resonant frequencies coincides with one of these transitions. Thus, a single molecular gain medium may be made to lase simply by tuning both the QCL to a specific IR frequency and the QPML cavity to the terahertz frequency of the transition. In this manner, any molecular rotational absorption transition may be made to lase, and millions of such transition frequencies have been measured or tabulated.[5–7]

Ammonia was the first molecule made to lase in this manner,[2] although not on rotational transitions but on widely spaced pure inversion transitions in the $\nu_2 = 1$ excited vibrational band. The pure inversion transition frequencies in $\nu_2 = 1$ are much larger than the well-known ground state microwave transitions (9–35 GHz), because the inversion energy is comparable to the height of the tunnel barrier. Consequently, the inversion splittings in $\nu_2 = 1$ are strong transitions clustered near 1.1 THz. A handful of such pure inversion laser transitions have been reported, including one that yielded 1 mW of output power, when a Q-branch ($J_L = J_U = J$) transition was pumped by a narrowly tunable QCL operating between 965 and 968 cm^{-1}.[3] More recently, additional lasing transitions pumped by IR transitions in NH_3 have been reported.[8,9]

By using a widely tunable pump source, we have demonstrated that the simple linear molecule nitrous oxide (N_2O) can achieve continuous-wave laser emission for at least 39 transitions with discrete line tunability from 0.25 to 0.95 THz.[1] More recently, we demonstrated

that using the prolate symmetric top molecule methyl fluoride (CH_3F) as the gain medium allows for even greater tunability with emission on at least 120 lines spanning 0.25–1.3 THz.[10]

In this Letter, we demonstrate the broad tunability that is possible from the ammonia QPML when rotation–inversion transitions are made to lase. We have discovered and characterized two multi-line lasing mechanisms in the ammonia QPML: simultaneous lasing of a pure inversion and a rotation–inversion transition sharing the same pumped upper level and cascaded lasing from a lower energy lasing transition indirectly connected to the pumped level. Both mechanisms allow simultaneous lasing at two very different frequencies, and in certain cases, the cascade mechanism allows for lasing at frequencies that would not otherwise be possible due to the selection rules.

It is well known that ammonia's rotational spectrum is complicated by the inversion splitting caused by the inversion tunneling of the nitrogen atom in this pyramidal molecule.[11,12] A simplified version of the energy level diagram for the ammonia molecule for $J \leq 3$ is given in Fig. 1(a), where the J is the quantum number representing the total angular momentum and K represents the projection of the angular moment along the symmetry axis of the molecule. Whether for pumping or lasing, the selection rules require a change in symmetry of the two energy levels associated with the inversion doublet, symmetric (s) and anti-symmetric (a), so the only allowed transitions are a → s or s → a. Consequently, pure inversion transitions and Q-branch transitions ($\Delta J = 0$) with $K = 0$ are forbidden. Because NH_3 is an oblate symmetric top, the lowest energy levels occur for $J = K$, and these are generally the most heavily populated.

Because of the inversion splitting, two types of P, Q, or R branch IR transitions may pump population into a given rotational state (J, K) within $\nu_2 = 1$ [see Fig. 1(b)]. The first (left side) is a higher energy transition connecting a lower symmetric inversion level in the ground vibrational state to a higher antisymmetric inversion level in $\nu_2 = 1$, denoted saP(J, K), saQ(J, K), or saR(J, K), respectively, spanning 679–948, 954–968, or 1007–1249 cm^{-1} for $0 \leq J \leq 14$. The converse transitions asP(J, K), asQ(J, K), and asR(J, K) (right side) occur at lower frequencies for a given J (respectively, 632–932, 905–949, or 952–1237 cm^{-1} for $0 \leq J \leq 14$).

The selection rules for a lasing transition are $\Delta J = 0, \pm 1$, $\Delta K = 0$, $s \leftrightarrow a$. Although "forbidden" transitions with $\Delta K = 3, 6, 9\ldots$ may be allowed,[13,14] their threshold for lasing will be higher than the $\Delta K = 0$ lines considered here. When an saQ(J, K) transition is pumped, two QPML direct lasing transitions may occur [shown on the left side of Fig. 1(b)]: the pure inversion transition $(J, K, a) \rightarrow (J, K, s)$ and the rotation–inversion transition $(J, K, a) \rightarrow (J-1, K, s)$. Because of symmetry-based selection rules, only sa pump transitions can directly produce lasing on pure inversion transitions. When an asQ(J, K) transition is pumped, the rotation–inversion transition $(J, K, s) \rightarrow (J-1, K, a)$ may be made to lase [the right side of Fig. 1(b)]. For simplicity, we label these three QPML transitions in $\nu_2 = 1$ as PI(J, K), RIas(J, K), and RIsa(J, K), respectively. Just as $J_U = J_L = J$ when a Q(J,K) transition is pumped, pumping an R(J, K) or P(J, K) transition may induce lasing on transitions with $J_U = J_L + 1$ or $J_U = J_L - 1$, respectively. In the following, we consider all three types of lasing transitions from Q or R branch pump transitions, both s → a and a → s.

To explore the relative tunability and efficacy of all three types of transitions systematically, we first compute the energy levels of ammonia as a function of J, K, and inversion state (a or s) using the published rotational constants for ammonia.[15] From these energy levels and the selection rules mentioned above, one can compute the expected direct lasing frequencies as a function of the pump wavenumber. For Q and R-branch IR pump transitions, QPML frequencies for representative transitions (those for which K is a multiple of 3) are plotted, respectively, in Figs. 2(a) and 2(b). These plots reveal that ammonia can be used as a gain medium in a widely tunable QPML spanning the frequency range 0.140–9.634 THz far beyond the limited tunability afforded by PI transitions clustered at 1.1 ± 0.3 THz.

How much power can be expected from these transitions? To understand how power depends on (J, K), we use the method described in our previous work[10] to compute the normalized slope efficiency and lasing threshold power for direct PI and RI lasing transitions of the ammonia laser. By eliminating the factors that depend on cavity geometry, pump power, and gas pressure, this calculation provides unitless quantities that allow line-by-line comparisons of the threshold and slope efficiency. The method requires computation of

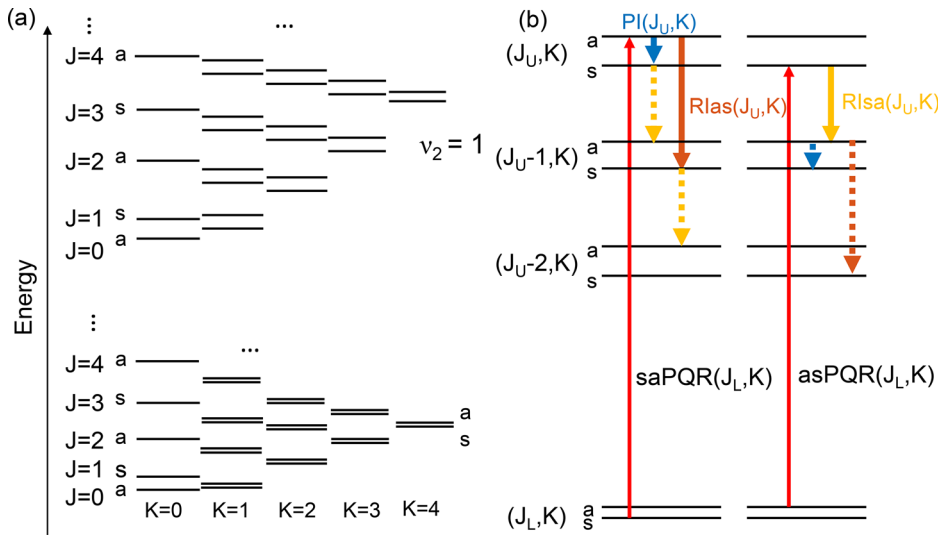

FIG. 1. (a) Energy level diagram of NH_3 in the ground and $\nu_2 = 1$ vibrational states. Note the alternating s and a levels at $K = 0$. (b) Three types of laser transitions are possible in NH_3 QPMLs: pure inversion (PI, blue) and rotation–inversion (RIas, red) when an s → a IR transition is pumped, and rotation–inversion (RIsa, yellow) for an a → s IR pump. Cascaded transitions for each type are illustrated as dashed arrows of the same colors.

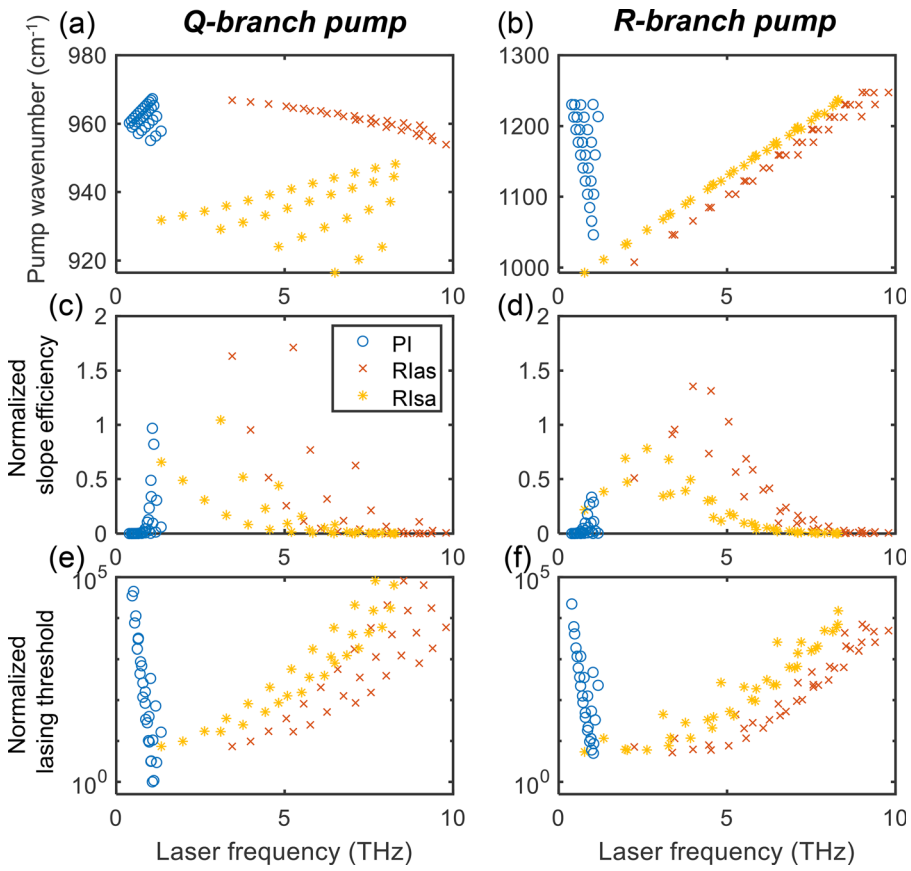

FIG. 2. Direct lasing transition frequencies for the NH_3 QPML, plotting only those transitions for which K is a multiple of 3, for (a) a Q-branch or (b) an R-branch pump. Normalized slope efficiency [(c) and (d)] and threshold [(e) and (f)] of the NH_3 QPML for those transitions using the method of Ref. 10 for a Q-branch [(c) and (e)] or an R-branch [(d) and (f)] pump.

the population fraction for each energy level and the branching ratios for both the pumped transition (P-, Q-, or R-branch) and the corresponding lasing transitions (PI, RIas, and RIsa) as a function of J, K, and inversion state.[11] Q-branch and pure inversion transitions are governed by a branching ratio that goes as K^2, while the R-branch and rotation–inversion transitions are governed by branching ratios that go as $(J+1)^2 - K^2$ and $J^2 - K^2$, respectively. Thus, Q-branch and pure inversion transitions are favored for large K, while R-branch and rotation–inversion transitions are favored for small K.

For Q-branch-pumped lasing transitions whose K is a multiple of 3, Figs. 2(c) and 2(e), respectively, give the slope efficiency and lasing threshold, normalized by the values for the lowest threshold line (pure inversion $J = 4, K = 3$). Similar plots are shown in Figs. 2(d) and 2(f) for an R-branch pump using the same normalization. With the exception of a few PI transitions, the transitions with the lowest threshold and highest slope efficiencies are RI transitions between 1 and 6 THz. The supplementary material for this manuscript includes a detailed explanation of the normalization process, followed by complete plots for all transitions and a table giving all the transition frequencies for $J_L \leq 10$.

To verify these predictions, we used the experimental setup depicted in Fig. 3(a). IR light from an external cavity (EC)-QCL (Daylight Solutions 41095-HHG-UT, tunable from 920 to 1194 cm^{-1}) is injected through a Brewster's angle ZnSe window into a THz cavity that consists of a 50 cm long copper pipe with a 4.8 mm internal diameter. A flat mirror in the front of the cavity with a centered 1 mm diameter pinhole is used as an output coupler. The cavity resonance frequency was tuned by changing the rear tuning mirror position to adjust the cavity length. A separate gas absorption cell containing 100 mTorr of anhydrous ammonia was used to monitor how precisely the QCL emission frequency was tuned to the desired NH_3 rovibrational transition.

Unlike previous demonstrations of the N_2O and CH_3F QPMLs, the rear mirror of the cavity can either be a flat mirror or a pinhole coupler (pinhole diameter 1.7 mm) sealed by a 4 mm thick polymethylpentene (TPX) window. The front ZnSe coupler absorbs light at frequencies above 2 THz, thereby acting as a low pass terahertz filter, while the TPX rear window transmits all terahertz frequencies. Outgoing terahertz light generated in the laser cavity can be collected from the front pinhole of the laser by an off-axis parabolic mirror and focused onto a detector using a 75 mm focal length TPX lens. However, the output power was greater when measured from the rear coupler with the larger pinhole and was not affected by the frequency dependent response of the ZnSe Brewster window or the hole in the off-axis parabolic mirror. Light from the rear of the cavity was characterized by a Tydex TSFPI-2 scanning Fabry–Pérot interferometer (SFPI) coupled with a broadband THz detector (Golay cell). The periodicity of interference fringes as a function of the path difference corresponds to the half-wavelength of the emitted light.

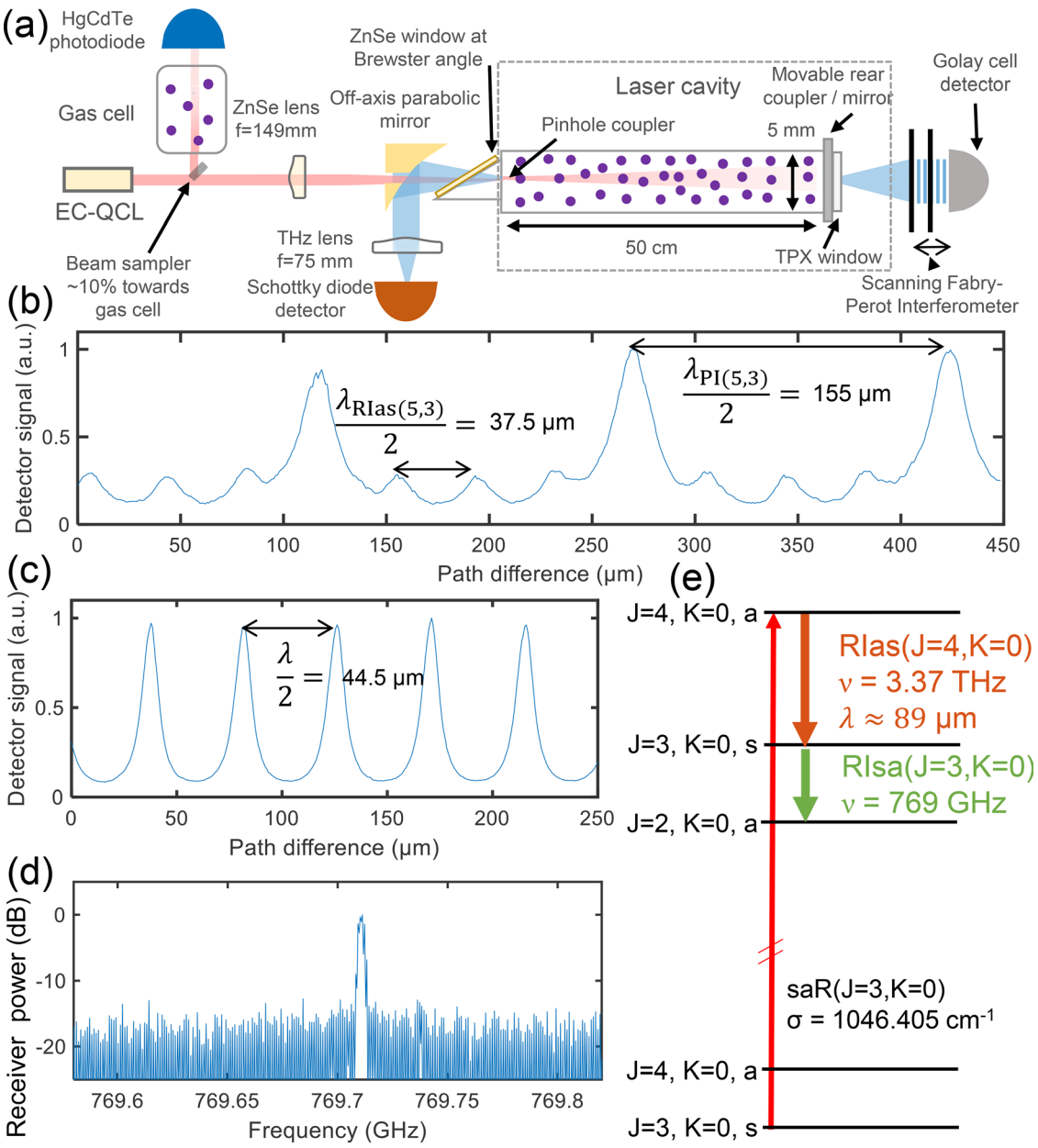

FIG. 3. (a) Experimental schematic of the NH_3 QPML: the 4.8 mm diameter and 50 cm long copper laser cavity has pinhole output couplers in the front and rear. (b) Interferogram measured with a scanning Fabry Perot inteferometer (SFPI), showing simultaneous lasing at ∼0.98 and ∼3.99 THz (wavelengths 310 and 75 μm). (c) Measured interferogram showing a laser emission frequency of ∼3.37 THz (89 μm wavelength). (d) Signal measured with a receiving mixer showing laser emission at 769.710 GHz. (e) Mechanism for simultaneous direct and cascaded laser emission in a NH_3 QPML pumped by the asR(3, 0) IR transition.

We pumped the QPML cell containing 20 mTorr of ammonia with the widely tunable QCL and measured 24 direct PI and RI lasing transitions spanning 0.769 710–4.458 880 THz by tuning the QCL across Q- and R-branch transitions from 966.269–967.407 and 992.699–1084.620 cm^{-1}, respectively. As can be seen in Fig. 1(b), either a pure inversion (blue solid arrow) or rotation–inversion (red solid arrow) transition may be made to lase. Surprisingly, when we pumped the saR(4, 3) IR transition at 1065.565 cm^{-1}, we observed both PI and RI lines to lase simultaneously. Figure 3(b), which plots the measured signal as a function of the path difference of the SFPI, exhibits two periodicities corresponding to simultaneous emission near 0.980 THz [PI(5, 3)] and 3.99 THz [RIas(5, 3)]. Without a spectrometer to discriminate these two lines, the total power emitted could have been mistakenly ascribed to just one of them. Experimentally, the relative

magnitude of each line can be adjusted by changing the cavity length and thereby tuning the cavity resonance to match either frequency.

We then pumped the same cell with the QCL tuned to the saR(3, 0) IR transition (1046.405 cm^{-1}), since the Q-branch version of this transition is forbidden. The pure inversion lasing transition is also forbidden for $K = 0$, because the (4,0,s) and (3,0,a) levels do not exist. The QPML could only lase on the RI transition, and light from that RIas(4,0) transition at 3.3736 THz was measured from the rear output coupler [solid red arrow in Fig. 1(b)]. The emission frequency was measured by the SFPI using the interferogram shown in Fig. 3(c).

Surprisingly, light was also measured from the front output coupler at 769.710 GHz using a receiving mixer (VDI SAX WR1.0) as shown in Fig. 3(d). According to the selection rules, calculated energy levels and published transition frequencies for ammonia[5–7,15,16] only direct lasing at 3.373 613 THz should be expected. The presence of light at two significantly different frequencies for the saR(3, 0) pump transition can be explained by the energy diagrams in Figs. 1(b) (yellow dashed arrow below solid red arrow) and 3(e). Molecules that mediated laser emission at 3.373613 THz [RIas(4, 0)] have relaxed to (3,0,s). At low gas pressures where collisional relaxation is very slow, these molecules in (3,0,s) created another population inversion above (2,0,a). This second population inversion can then emit light at the RIsa(3, 0) frequency once it reaches the lasing threshold, which is what was observed. Note that this cascaded transition, measured at 769.710 GHz, is not the diagonal transition near 772.595 GHz caused by an accidental $\Delta K = 3$ degeneracy first reported by Belov *et al.*[13]

Unlike the situation shown in Fig. 3(b), the SFPI interferogram in Fig. 3(c) does not exhibit a second periodicity at half the wavelength of the cascaded line (195 μm). This shows that the power emitted at the cascaded line is much lower than the direct frequency. We measured the output power of the laser emitting around 3.37 THz using a calibrated calorimeter detector (VDI PM5B) combined with a conical horn matched with the waveguide input of the power meter. We placed the conical horn right in front of the rear TPX window and measured an output power as large as 0.45 mW in this configuration. (In the supplementary material, we plot the measured beam profile.) Because of its magnitude, we can attribute at least 95% of this output power to the direct line lasing at 3.373 613 THz. After accounting for

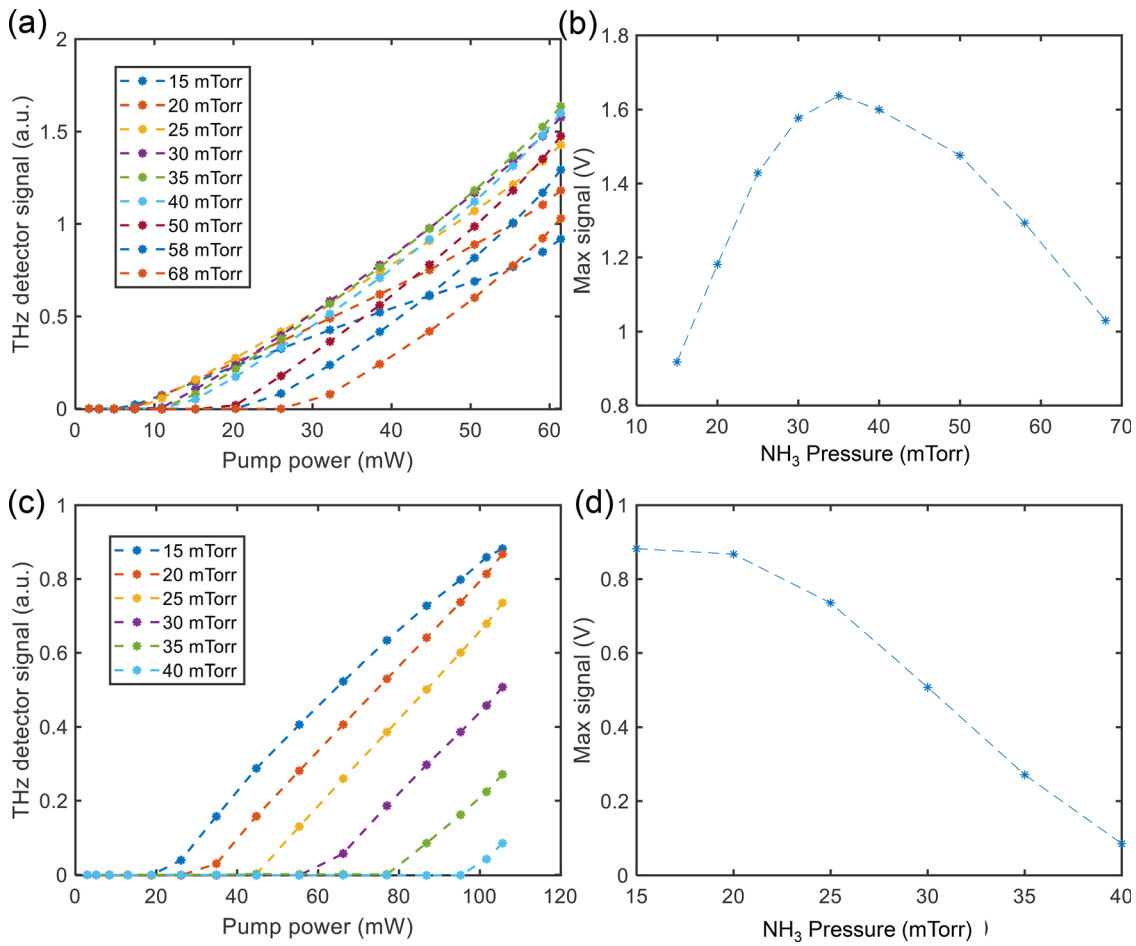

FIG. 4. (a) Plot of the detected signal at 769.710 GHz for an infrared pump at 992.699 cm^{-1} (direct lasing line) as a function of the pump power and gas pressure. (b) Plot of the peak signal from (a) as a function of the gas pressure. (c) Plot of the detected signal at 769.710 GHz for an infrared pump at 1046.405 cm^{-1} (cascaded lasing line) as a function of the pump power and gas pressure. (d) Plot of the peak signal from (c) as a function of the gas pressure.

TABLE I. Table giving the frequency of measured cascaded lines along with their direct pump wavenumber.

Frequency (GHz)	Transition type	Direct R pump wavenumber (cm^{-1})	Cascaded R pump wavenumber (cm^{-1})	Direct Q pump wavenumber (cm^{-1})
769.710	RIsa(3,0)	asR(2,0) @ 992.699	saR(3,0) @ 1046.405	Not allowed
762.852	RIsa(3,1)	asR(2,1) @ 992.450	saR(3,1) @ 1046.401 or saR(2,1) @ 1027.047	asQ(3,1) @ 967.449
1393.079	RIsa(4,1)	asR(3,1) @ 1013.176	saR(4,1) @ 1065.594 or saR(3,1) @ 1046.401	asQ(4,1) @ 967.031
1073.050	PI(3,3)	Not allowed	asR(3,3) @ 1011.204	asQ(3,3) @ 967.346
1030.530	PI(4,3)	saR(3,3) @ 1046.375	asR(4,3) @ 1032.131	asQ(4,3) @ 966.905
979.650	PI(5,3)	saR(4,3) @ 1065.565	asR(5,3) @ 1053.130	asQ(5,3) @ 966.380

the Manley–Rowe factor,[1] the internal quantum efficiency for converting IR photons into THz photons is approximately 2.8% for this transition and may be as large as 11% (1.8 mW output) if absorption and reflection from the collection optics introduce as much as a factor of four loss from emission to detection.

In order to confirm cascaded lasing, we measured the detected signal at 769.710 GHz as a function of the pump power and ammonia pressure for both the direct RI transition [pumped by asR(2, 0) at 992.699 cm^{-1}] and the cascaded line [pumped by saR(3, 0)], and the results are plotted in Figs. 4(a) and 4(c). These measurements were both conducted using a flat mirror instead of a pinhole coupler at the rear of the cavity in order to lower the radiative cavity losses. Although the output power obtained through the front coupler was significantly reduced, we, nevertheless, observe that the cascaded lasing threshold is higher than the direct lasing threshold, an indication of different excitation mechanisms.

As further confirmation of the different excitation mechanisms, we measured the peak signal as a function of NH_3 gas pressure using the maximum available pump power for the respective pump frequencies (89 mW at 992.699 cm^{-1} and 152 mW at 1046.405 cm^{-1}). Figures 4(b) and 4(d) reveal that cascaded lasing is more efficient at low pressures, reaching its maximum power at 15 mTorr, while direct lasing is more efficient at higher pressures, reaching its maximum power at 30 mTorr.

This *cascaded* lasing, as opposed to *direct* lasing, has been seen on a few transitions in other optically pumped far-IR laser gases at low pressures and high pump powers.[17,18] However, with tunable QCLs, this cascaded lasing at low pressures is possible on most transitions in most molecules, including ammonia. As summarized in Table I, we observed cascaded lasing on six lines, including lines for which $K \neq 0$ so that PI transitions are also allowed. For example, when pumping on the saR(3, 1) IR transition, we observed both cascaded lasing at 762.852 GHz, corresponding to the RIsa(3, 1) line, and direct lasing at 973.827 GHz, corresponding to the PI(4, 1) line, just by appropriately tuning the cavity resonance. Because of the low K value, the threshold of the PI line was larger than the threshold of the cascaded transition. In general, the choice of the K value is particularly important to determine which type of cascaded line can be made to lase. As noted above, pure inversion transitions are favored for large K while rotation–inversion transitions are favored for small K. Thus, by choosing K close to 0, the threshold of any pure inversion line is significantly increased, so direct or cascaded lasing is more likely to happen on a rotation inversion line. Conversely, by choosing K close to J, PI transitions will have a lower lasing threshold and will be more likely to be observed as direct or cascaded transitions.

From these observations, it has become apparent that two types of simultaneous multi-line lasing transitions—multiple direct and direct-cascaded—exist in ammonia [see Fig. 1(b)]. Specifically, the saPQR (J_L, K) pump can generate simultaneous lasing on two direct transitions, PI (J_U, K) and RIas (J_U, K), each of which can produce lasing on a different cascaded laser transition, RIsa (J_U, K) and RIsa $(J_U - 1, K)$, respectively. By contrast, the asPQR (J_L, K) pump can create only one direct transition, RIas (J_U, K), but it can produce two cascaded lasing transitions, PI $(J_U - 1, K)$ and RIas $(J_U - 1, K)$. In either case, which lines actually lase is determined by the transition-unique branching ratios, energy levels, and cavity tuning, but it is possible that up to four or three lines of significantly different frequencies may lase simultaneously in the former or latter cases, respectively. In all, 34 lasing transitions were observed, spanning 0.762 852 to 4.458 880 THz (see the supplementary material for details), including seven that were observed through multiple excitation pathways. This multi-line lasing attribute adds further excitement to the ammonia QPML, whose unique energy level spectrum permits broad single line tunability from 0.140 to at least 9.634 THz.

See the supplementary material for additional details about the experimental and theoretical works presented in this paper.

The authors acknowledge S. Cotreau and A. DiMambro of Harvard University Instructional machine shop for their help with fabrication of the THz cavity elements. This work was partially supported by the U.S. Army Research Office (Contract Nos. W911NF-19-2-0168 and W911NF-20-1-0157) and DRS Daylight Solutions. Any opinions, findings, conclusions, or recommendations expressed in this material are those of the authors and do not necessarily reflect the views of the Assistant Secretary of Defense for Research.

AUTHOR DECLARATIONS

Conflict of Interest

The authors declare no conflicts of interest.

DATA AVAILABILITY

The data that support the findings of this study are available from the corresponding authors upon reasonable request.

REFERENCES

[1]P. Chevalier, A. Amirzhan, F. Wang, M. Piccardo, S. G. Johnson, F. Capasso, and H. O. Everitt, "Widely tunable compact terahertz gas lasers," Science **366**, 856–860 (2019).

[2]A. Pagies, G. Ducournau, and J.-F. Lampin, "Low-threshold terahertz molecular laser optically pumped by a quantum cascade laser," APL Photonics **1**, 031302 (2016).

[3]J.-F. Lampin, A. Pagies, G. Santarelli, J. Hesler, W. Hansel, R. Holzwarth, and S. Barbieri, "Quantum cascade laser-pumped terahertz molecular lasers: Frequency noise and phase-locking using a 1560 nm frequency comb," Opt. Express **28**, 2091–2106 (2020).

[4]F. Wang, J. Lee, D. J. Phillips, S. G. Holliday, S.-L. Chua, J. Bravo-Abad, J. D. Joannopoulos, M. Soljačić, S. G. Johnson, and H. O. Everitt, "A high-efficiency regime for gas-phase terahertz lasers," Proc. Natl. Acad. Sci. U. S. A. **115**, 6614–6619 (2018).

[5]P. Chen, T. J. Crawford, B. J. Drouin, J. C. Pearson, S. Yu, Sung, and D. Nemchick (2017). "JPL molecular spectroscopy database," Jet Propulsion Lab. https://spec.jpl.nasa.gov/.

[6]A. J. Remijan, A., Markwick-Kemper, and ALMA Working Group on Spectral Line Frequencies, "Splatalogue database for astornomical spectroscopy," in *American Astronomical Society, AAS Meeting 211, Bulletin of the American Astronomical Society* (AAS, 2007), Vol. 39, p. 963; available at splatalogue. https://splatalogue.online//.

[7]I. E. Gordon, L. S. Rothman, R. J. Hargreaves, R. Hashemi, E. V. Karlovets, F. M. Skinner, E. K. Conway, C. Hill, R. V. Kochanov, Y. Tan, P. Wcisło, A. A. Finenko, K. Nelson, P. F. Bernath, M. Birk, V. Boudon, A. Campargue, K. V. Chance, A. Coustenis, B. J. Drouin, J.-M. Flaud, R. R. Gamache, J. T. Hodges, D. Jacquemart, E. J. Mlawer, A. V. Nikitin, V. I. Perevalov, M. Rotger, J. Tennyson, G. C. Toon, H. Tran, V. G. Tyuterev, E. M. Adkins, A. Baker, A. Barbe, E. Canè, A. G. Császár, A. Dudaryonok, O. Egorov, A. J. Fleisher, H. Fleurbaey, A. Foltynowicz, T. Furtenbacher, J. J. Harrison, J.-M. Hartmann, V.-M. Horneman, X. Huang, T. Karman, J. Karns, S. Kassi, I. Kleiner, V. Kofman, F. Kwabia-Tchana, N. N. Lavrentieva, T. J. Lee, D. A. Long, A. A. Lukashevskaya, O. M. Lyulin, V. Y. Makhnev, W. Matt, S. T. Massie, M. Melosso, S. N. Mikhailenko, D. Mondelain, H. S. P. Müller, O. V. Naumenko, A. Perrin, O. L. Polyansky, E. Raddaoui, P. L. Raston, Z. D. Reed, M. Rey, C. Richard, R. Tóbiás, I. Sadiek, D. W. Schwenke, E. Starikova, K. Sung, F. Tamassia, S. A. Tashkun, J. Vander Auwera, I. A. Vasilenko, A. A. Vigasin, G. L. Villanueva, B. Vispoel, G. Wagner, A. Yachmenev, and S. N. Yurchenko, "The HITRAN2020 molecular spectroscopic database," J. Quant. Spectrosc. Radiat. Transfer **277**, 107949 (2022).

[8]M. Wienold, A. Zubairova, and H.-W. Hübers, "Laser emission at 4.5 THz from $^{15}NH_3$ and a mid-infrared quantum-cascade laser as a pump source," Opt. Express **28**, 23114–23121 (2020).

[9]M.-H. Mammez, Z. Buchanan, O. Pirali, M.-A. Martin-Drumel, J. Turut, G. Ducournau, S. Eliet, F. Hindle, S. Barbieri, P. Roy *et al.*, "Optically pumped terahertz molecular laser: Gain factor and validation up to 5.5 THz," Adv. Photonics Res. **2022**, 2100263.

[10]A. Amirzhan, P. Chevalier, J. Rowlette, H. T. Stinson, M. Pushkarsky, T. Day, H. O. Everitt, and F. Capasso, "A quantum cascade laser-pumped molecular laser tunable over 1 THz," APL Photonics **7**, 016107 (2022).

[11]W. Gordy, R. L. Cook, and A. Weissberger, *Microwave Molecular Spectra* (Wiley, New York, 1984), Vol. 18.

[12]C. H. Townes and A. L. Schawlow, *Microwave Spectroscopy* (Dover Publications, 1975).

[13]S. Belov, L. Gershstein, A. Krupnov, A. Maslovskij, Š. Urban, V. Špirko, and D. Papoušek, "Inversion and inversion-rotation spectrum of $^{14}NH_3$ in the ν_2 excited state," J. Mol. Spectrosc. **84**, 288–304 (1980).

[14]T. Oka, "Forbidden rotational transitions and astrophysics," J. Mol. Spectrosc. **379**, 111482 (2021).

[15]S. Yu, J. C. Pearson, B. J. Drouin, K. Sung, O. Pirali, M. Vervloet, M.-A. Martin-Drumel, C. P. Endres, T. Shiraishi, K. Kobayashi *et al.*, "Submillimeter-wave and far-infrared spectroscopy of high-J transitions of the ground and $\nu_2 = 1$ states of ammonia," J. Chem. Phys. **133**, 174317 (2010).

[16]J. C. Pearson, S. Yu, and O. Pirali, "Modeling the spectrum of the $2\nu_2$ and ν_4 states of ammonia to experimental accuracy," J. Chem. Phys. **145**, 124301 (2016).

[17]T. Chang, T. Bridges, and E. Burkhardt, "CW laser action at 81.5 and 263.4 μm in optically pumped ammonia gas," Appl. Phys. Lett. **17**, 357–358 (1970).

[18]K. J. Button, *Reviews of Infrared and Millimeter Waves: Volume 2 Optically Pumped Far-Infrared Lasers* (Springer Science & Business Media, 2013).